ACS APPLIED MATERIALS & INTERFACES

Research Article

www.acsami.org

Facile Synthesis of Poly(3,4-ethylenedioxythiophene) Film via Solid-State Polymerization as High-Performance Pt-Free Counter Electrodes for Plastic Dye-Sensitized Solar Cells

Xiong Yin,[†,∥] Fan Wu,[†,§,∥] Nianqing Fu,[‡,∥] Jing Han,[‡] Dongliang Chen,[§] Peng Xu,[†] Meng He,*[,†] and Yuan Lin*[,‡]

[†]National Center for Nanoscience and Technology, Beijing 100190, P. R. China

[‡]Key Laboratory of Photochemistry, Beijing National Laboratory for Molecular Sciences (BNLMS), Institute of Chemistry, Chinese Academy of Sciences, Beijing 100190, P.R. China

[§]College of Mechanical and Electrical Engineering, Beijing University of Chemical Technology, Beijing 100029, P.R. China

ABSTRACT: A high-performance Pt-free counter electrode (CE) based on poly(3,4-ethylenedioxythiophene) (PEDOT) film for plastic dye-sensitized solar cells (DSCs) has been developed via a facile solid-state polymerization (SSP) approach. The polymerization was simply initiated by sintering the monomer, 2,5-dibromo-3,4-ethylenedioxythiophene (DBEDOT), at the temperature of 80 °C, which can be applied on the plastic substrate. The cyclic voltammetry measurements revealed that the catalytic activity of the SSP-PEDOT CE for triiodide reduction is comparable with that of the Pt CE. Under optimized conditions, the power conversion efficiency of a DSC with a N719-sensitized TiO_2 photoanode and the SSP-PEDOT CE is 7.04% measured under standard 1 sun illumination (100 mW cm^{-2}, AM 1.5), which is very close to that of the device fabricated under the same conditions with a conventional thermally deposited Pt CE (7.35%). Furthermore, taking advantage of the compatibility of the SSP-PEDOT with the plastic substrates, a full plastic N719-sensitized TiO_2 solar cell was demonstrated, and an efficiency of 4.65% was achieved, which is comparable with the performance of a plastic DSC with a sputter-deposited Pt CE (5.38%). These results demonstrated that solid-state polymerization initiated at low temperature is a facile and low-cost method of fabricating the high-performance Pt-free CEs for plastic DSCs.

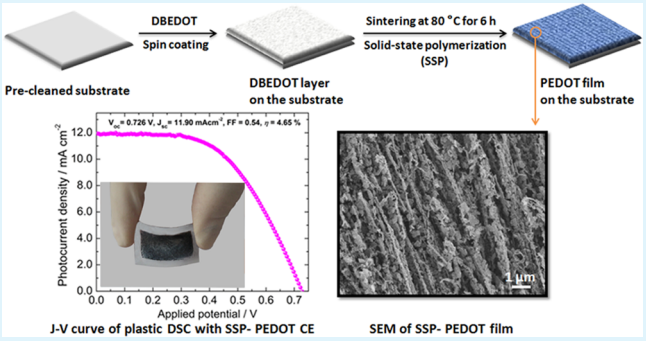

KEYWORDS: *2,5-dibromo-3,4-ethylenedioxythiophene, solid-state polymerization, plastic substrate, poly(3,4-ethylenedioxythiophene), flexible dye-sensitized solar cells, electrochemical impedance spectra*

INTRODUCTION

Dye-sensitized solar cells have been considered as a potential alternative to conventional p−n junction solar cells because of their low-cost production, simple fabrication process, and relatively high energy conversion efficiency.[1−3] After having been investigated for more than 20 years, liquid-state type DSCs with an efficiency as high as 12.3% have been demonstrated.[4] Typically, the conventional liquid-state DSC consists of a dye-sensitized porous semiconductor photoanode, liquid electrolyte containing a redox couple, and a counter electrode.[1] The triiodide/iodide redox species are commonly utilized as the redox couple in the liquid-state DSC due to its unique performance on regeneration of various sensitizers including organic dyes[5,6] and Ru-based dyes.[7] The functions of the counter electrode are to collect electrons from the external circuit, transfer electrons back to the redox couple, and catalyze the redox couple at the counter electrode/electrolyte interface.[8,9] To obtain high conversion efficiency, the counter electrode materials, therefore, should possess high electrical conductivity and superior electrocatalytic activity to decrease the overvoltage for minimizing the energy losses. Noble metal platinum is widely used as the counter electrode in DSCs due to its high electrocatalytic property for triiodide reduction. However, the dissolution of Pt film in the liquid-state I_3^-/I^- electrolyte to generate PtI_4 will show a negative effect on the long-term performance of the DSC device.[10] Moreover, Pt is expensive, and its resources are rather limited, which hinders its large-scale applications.[11−13] In addition, the conventional fabrication of a Pt CE commonly involves the high-temperature sintering process, which prohibits its application on plastic polymer substrates as plastic substrates can only sustain temperature lower than 150 °C.[14−18] Furthermore, compared with rigid DSCs based on the glass substrate, plastic DSCs are thin, lightweight, and flexible. More importantly, plastic DSCs

Received: May 8, 2013
Accepted: August 8, 2013
Published: August 8, 2013

   dx.doi.org/10.1021/am401719e | ACS Appl. Mater. Interfaces 2013, 5, 8423−8429

can be produced on a large scale with roll-to-roll techniques.[19] Therefore, a lot of effort has been devoted to the development of the low-cost alternative materials for Pt with good compatibility with the plastic substrate. Recently, different kinds of CEs have been developed for DSCs, including metallic compounds,[20−22] carbon-based materials,[23−25] and conducting polymers.[11−13,26−28] Most of these materials possess comparable electrocatalytic performances for triiodide reduction with that of Pt in DSC devices. Poly(3,4-ethylenedioxythiophene) (PEDOT), one kind of conducting polymer, has attracted much research attention due to its ease of processing with remarkable stability, electrical conductivity, and catalytic capability, compared with other conducting polymers.[29] In addition, composite films based on PEDOT can be easily fabricated on a plastic substrate, indicating that they are very attractive alternatives of Pt CE.

The reported PEDOT CEs have been usually prepared using chemical polymerization[30,31] and electro-polymerization techniques.[26] The reaction initiators, unreacted monomers, and other chemicals involved in the chemical polymerization can reduce the conductivity of the as-prepared film, which showed a negative effect on the catalytic activity of a polymer CE for triiodidie reduction.[30,31] In addition, these residues in the PEDOT films will occupy the reaction sites for the catalytic process, which also leads to a negative effect on catalytic activity.[31] Therefore, prior to fabricating the counter electrodes, these films need to be carefully rinsed with water and other solvents. Electro-polymerization has been widely used in the direct formation of conducting polymers onto fluorine-doped tin oxide (FTO) or ITO conducting surfaces. More recently, the PEDOT films or composite films have been prepared using various electrochemical techniques, including constant current[26] and potentiostatic mode.[28] Additionally, the morphologies and properties of the resultant films are largely dependent on the electrochemical methods and supporting electrolytes used in the study.[26,28] The resultant PEDOT films were in the oxidized form with various counterpart anions due to the electro-polymerization process. As demonstrated in the previous reports, fabrication technique also plays a decisive role in determining the quality of the as-prepared materials.[26−28,30,31]

The solid-state reaction is widely used in the preparation of polycrystalline solids[32,33] and conducting polymer[34,35] with advantages of environmental friendliness, economics, and relatively high yield. Solid-state polymerization (SSP) is a catalyst-free cross-coupling reaction without solvent, and it is a facile method for polymerization of suitable monomer species.[34,35] SSP of well-ordered halogenated crystalline heterocyclic monomers can yield highly conductive polymers. In the present study, we report that highly efficient PEDOT CEs for rigid and plastic DSC devices can be easily obtained via a solid-state polymerization using 2,5-dibrominated-3,4-ethylenedioxythiophene (DBEDOT) as the monomer. The polymerization reaction was initiated simply by heating at the low temperature, without adding any catalysts, leading to the formation of the PEDOT film with well-defined polymer structure, which will benefit the catalytic reduction for triiodide. The electrocatalytic effect of SSP-PEDOT CEs on the redox couples were investigated using cyclic voltammetry. The DSC fabricated with N719-sensitized TiO_2 as the photoanode and SSP-PEDOT as the CE on a rigid FTO substrate and plastic substrate showed a high conversion efficiency of 7.04% and 4.65% under standard AM 1.5 sunlight illumination, respectively. The conversion efficiencies are comparable to that of a DSC device based on the thermally deposited Pt CE and sputter-deposited Pt CE, respectively. The results demonstrated that solid-state polymerization is a facile method to manufacture a PEDOT CE with superior photovoltaic performance for plastic devices.

EXPERIMENTAL SECTION

Materials. 3,4-Ethylenedioxythiophene, *N*-bromosuccinimide, 4-*tert*-butylpyridine (TBP), and iodine (I_2) were purchased from Sigma-Aldrich. Acetonitrile, chloroform, titanium tetrachloride ($TiCl_4$), and sodium bicarbonate were bought from Aladdin Industrial Inc. All chemicals and solvents used were of analytical grade, and they were used without further purification. Conducting FTO glass (sheet resistance: 15 Ω sq^{-1}, Nippon Sheet Glass Co., Japan) and a plastic ITO/PEN sheet (sheet resistance: 25 Ω sq^{-1}, Kintec Co., Hongkong) were used as the electrode substrates.

Synthesis of 2,5-Dibromo-3,4-ethylenedioxythiophene (DBEDOT). 2,5-Dibromo-3,4-ethylenedioxythiophene (DBEDOT) monomer was synthesized according to the previous reports with minor modifications.[36] In brief, 1.5 g of 3,4-ethylenedioxythiophene was first dissolved in a solution of 30 mL of $CHCl_3$ and 30 mL of glacial acetic acid. Then, 6 g of *N*-bromosuccinimide was slowly added into the above-mentioned solution at 0−5 °C under a nitrogen atmosphere. After it was stirred at room temperature for another 4 h, the solution was then poured into 200 mL of distilled water. The green-blue organic layer was separated, and the water layer was extracted with chloroform (50 mL × 3). The combined organic layer was washed again with 100 mL of distilled water. The organic layer was neutralized with sodium bicarbonate and then filtered. The solvent was then removed under vacuum by rotary evaporation. The dark blue solid product was purified using column chromatography with CH_2Cl_2 and petroleum ether (1:1) as eluent to get white crystals in 70% yield. ^1H NMR ($CDCl_3$): (4.4 ppm, s, CH_2). ^{13}C NMR ($CDCl_3$): 140.3, 84.6, 65.1 ppm.

Preparation of Counter Electrodes. The PEDOT CEs were prepared on precleaned rigid fluorine-doped tin oxide (FTO) glass substrate and plastic ITO/PEN substrate. The DBEDOT monomer solution was spin-coated onto these substrates (600 rpm for 15 s, which is followed by 1000 rpm for 30 s). Then, it was naturally dried to evaporate organic solvent and subsequently sintered at 80 °C for 6 h at an ambient atmosphere. Heating the DBEDOT monomer at 80 °C can produce a highly conducting polymer film in a relatively short time, according to previous reports.[34,35] The PEDOT film on a rigid substrate or plastic substrate was obtained via the solid-state polymerization process. The loading amount of PEDOT on the substrate was controlled by adjusting the concentration of the DBEDOT monomer in the $CHCl_3$. To optimize the photovoltaic performance of SSP-PEDOT CE based devices, three samples with different loading amount of PEDOT films, namely, PEDOT-1 (1.5 mg cm^{-2}), PEDOT-2 (3.0 mg cm^{-2}), and PEDOT-3 (4.5 mg cm^{-2}), were tested. For comparison, traditional Pt CEs were also prepared using spin-coating of 5 mM chloroplatinic acid solution on rigid FTO substrate followed by sintering at 385 °C for 30 min. A sputter coater was utilized to deposit a Pt thin layer on the plastic PEN/ITO substrate to obtain the sputter-deposited Pt CE used in the plastic devices.

Fabrication of DSC Device. A rigid TiO_2 electrode consisting of a transparent TiO_2 layer with thickness of 14 μm and a 4 μm TiO_2 scattering layer was prepared by doctor-blading a corresponding paste of TiO_2 nanoparticles from Solaronix (Ti-Nanoxide HT/SP) and Dyesol (WER4-O) onto FTO glass substrates. The electrodes were heated on a hot plate (Fischer) in an air atmosphere at 125 °C (10 min), 225 °C (10 min), 325 °C (20 min), 375 °C (20 min), and 450 °C (30 min). A $TiCl_4$ treatment was performed by treating the electrodes at 70 °C in 40 mM $TiCl_4$ solution for 30 min. The electrode was then subsequently washed with water and ethanol. Finally, the electrode was sintered at 450 °C for 30 min and allowed to cool to 85 °C before immersion in 0.5 mM N719 dye solution (mixture of

acetonitrile/*tert*-butanol with volume ration of 1:1) for dye absorbing. A flexible TiO_2 photoanode on plastic PEN/ITO substrate was prepared using the electrophoretic deposition (EPD) method according to our previous reports.[16] The thickness of plastic P25 TiO_2 electrode was about 11 μm. Prior to soaking in N719 dye solution, the flexible TiO_2 photoanode was heated at 85 °C for 30 min. After sensitizing with the dye, the electrode was rinsed with dry acetonitrile and then dried under a high-purity nitrogen stream. A 25 μm thick Surlyn thermoplastic film was used to separate the N719-sensitized TiO_2 photoanodes and counter electrodes. The space between the electrodes was filled with liquid electrolyte consisting of 0.4 M LiI, 0.04 M tetrabutylammonium iodide, 0.3 M 4-*tert*-butylpyridine, and 0.04 M I_2 in 3-methyoxypropionitrile.

Characterization and Measurement. The detailed morphologies of the DBEDOT monomer and PEDOT were observed with a field emission scanning electron microscope (FE-SEM, S4800, Hitachi). The electrochemical characterizations of CEs were evaluated by cyclic voltammetry measurement (CV). CV was conducted using a potentiostat (CHI630E, CHI instruments) with a three-electrode system in an acetonitrile solution containing 10 mM LiI, 1 mM I_2, and 0.1 M $LiClO_4$ at a scanning rate of 50 mV s^{-1}. The as-prepared CE, Ag/AgCl electrode, and Pt foil were used as working electrode, reference electrode, and counter electrode, respectively. Electrochemical impedance spectra (EIS) of the CEs were performed on dummy cells with two identical electrodes using a frequency response analyzer (Solartron SI 1270) and a potentiostat (Solartron 1287) at bias of 0 V with amplitude of 10 mV in the frequency range from 0.05 to 100 000 Hz. EIS measurements of DSCs were conducted using the same response analyzer and potentiostat at an amplitude of 10 mV and the open-circuit voltage under 100 mW cm^{-2} illumination in the frequency range from 0.05 to 100 000 Hz. The photocurrent−voltage (I−V) characteristics of the DSC devices were measured under AM 1.5G illumination (100 mW cm^{-2}) using an Oriel Newport solar simulator equipped with a 300 W xenon lamp and a digital source meter (2420, Keithley Instruments, USA). The light intensity was calibrated using a standard Si reference solar cell (Oriel PN 91150 V).

RESULTS AND DISCUSSION

The thin films of DBEDOT and PEDOT were prepared on the substrates using the spin-coating method without or with sintering post-treatment, respectively, and photographs and surface morphologies of the resultant films are shown in Figure 1. The DBEDOT monomer particles are uniformly distributed on the substrate (Figure 1a). After being heated at 80 °C for 6 h, the colorless DBEDOT crystal transformed into a dark blue material (PEDOT). SEM images of higher magnification revealed a significant change of the surface morphology. The PEDOT film shows a rough surface composed of nanostructures, which we believe will benefit the triiodide reduction. In addition, the surface of the PEDOT film exhibits a stripe-like microstructure which might result from the formation of the polymer chain during the polymerization process.[34,35]

To understand the catalytic mechanism of CEs, the electrochemical behaviors of CEs toward the I_3^-/I^- redox reaction were studied by cyclic voltammogram analysis.[18] Figure 2 shows the CV curves of PEDOT and Pt electrodes in the acetonitrile solution containing $LiClO_4$ as the supporting electrolyte and LiI and I_2 as the redox couple. Two typical pairs of oxidation/reduction peaks were obviously observed for the two CEs. It is well-known that the redox pair at relatively positive potentials is attributed to redox reaction 1, whereas the redox pair at the much more negative potentials is assigned to the redox reaction 2[26−28]

$$3I_2 + 2e = 2I_3^- \quad (1)$$

$$I_3^- + 2e = 3I^- \quad (2)$$

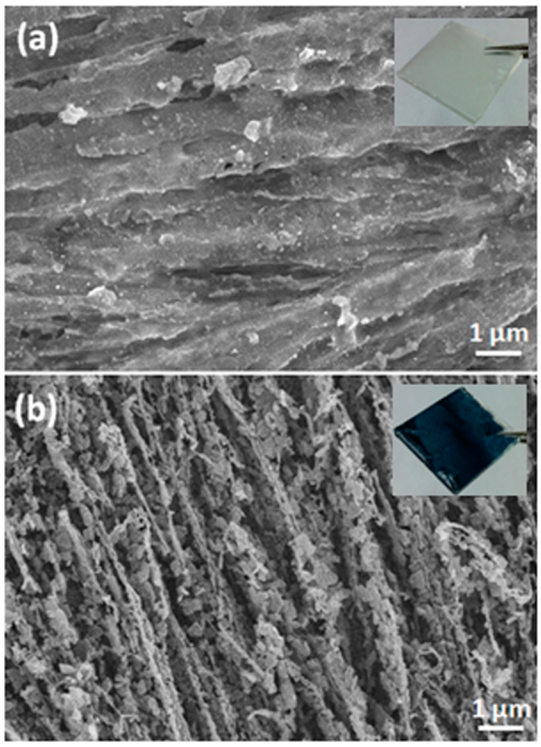

Figure 1. Photographs and FESEM images of DBEDOT (a) and PEDOT (b) film fabricated via solid-state polymerization on the FTO substrate.

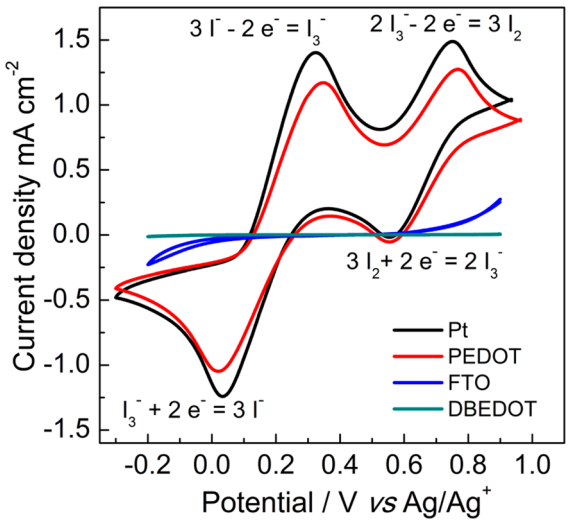

Figure 2. Cyclic voltammograms of DBEDOT, PEDOT (3.0 mg cm^{-2}), FTO, and Pt electrodes at a scan rate of 50 mV s^{-1} in 10 mM LiI, 1 mM I_2 solution containing 0.1 M $LiClO_4$ as the supporting electrolyte.

In the DSC, the photooxidized dyes are regenerated by I^- ions, while I^- ions are oxidized to I_3^-. The produced I_3^- ions are reduced to I^- at the CE interface. Therefore, the reduction peak of reaction 2 is the research focus of CV analysis.[12] The cathodic peak potential and peak current density shown for the PEDOT-based electrode are very close to those of the Pt electrode. These results also indicate that the PEDOT electrode can electrocatalyze the I_3^-/I^- redox couple as effectively as the Pt electrode. In addition, the shape of the CV curve of PEDOT prepared by the solid-state polymerization method is similar to

those of PEDOT prepared by electrochemical and chemical methods.[26−28,30,31] It also demonstrates that solid-state polymerization is an efficient method to synthesize high-performance PEDOT films. For comparison, the corresponding CV measurements of the blank FTO electrode and DBEDOT monomer film were also conducted. Obviously, the blank FTO electrode and DBEDOT monomer electrode show no electrocatalytic activity for the reduction of triiodide ions. The CVs of the FTO and DBEDOT monomer film did not present the characteristic peaks of the redox process. The current density of DBEDOT monomer film is even smaller than that of the blank FTO electrode. This is mainly ascribed to poor conductivity of DBEDOT monomer film. It reveals that the DBEDOT film acts as an insulator layer in the study, which suppresses the transfer of electrons from FTO to I_3^-/I^- redox couple in the solution. Thus, it is necessary to form a conducting polymer PEDOT via a facile solid-state polymerization process for effective I_3^- reduction.

EIS measurement was further carried out to analyze the electrochemical characteristics of different counter electrodes.[37] The EIS measurements were conducted on a symmetric sandwich cell configuration assembling with two identical electrodes. Figure 3 presents the Nyquist plots of the Pt and

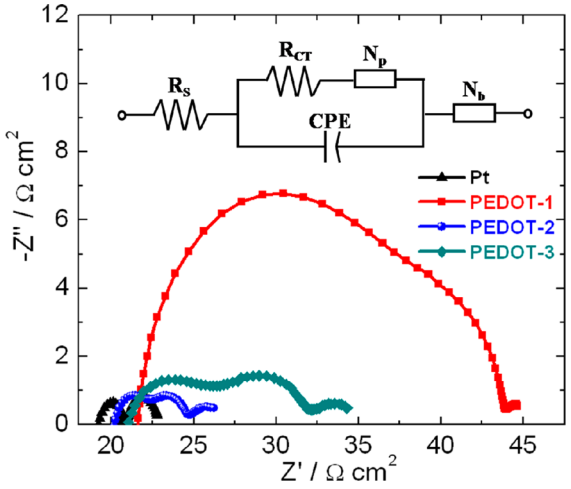

Figure 3. Nyquist plots for electrochemical impedance spectra of the symmetrical cells with two identical counter electrodes; inset shows the corresponding equivalent circuit.

PEDOT CEs. Two semicircles were observed in the case of a Pt CE, while three semicircles were observed for PEDOT CEs. Three semicircles in the EIS for two identical electrodes were also found in the graphene-based materials[38] and PEDOT-based composite CEs.[21] According to the previous reports, the presence of three semicircles is due to the porous structures of the material used to prepare CEs.[21,38] Meanwhile, the semicircle in the high-frequency region is ascribed to the Nernst diffusion impedance (N_P) resulting from diffusion through the electrode pores. The middle-frequency semicircle corresponds to the charge transfer resistance (R_{CT}) and the double-layer capacitance (CPE) of the electrode surface. The low-frequency semicircle is determined by bulk Nernst diffusion (N_b) of the redox couple in the electrolyte. The intercept on the real axis in the high-frequency region is assigned to the series resistance of the cell (R_S). The equivalent circuit used for PEDOT CEs is shown in the inset of Figure 3. The corresponding fitting data of R_S, R_{CT}, and N_P are summarized in Table 1. Three PEDOT CEs exhibited nearly identical R_S values (about 21 Ω cm^2). However, R_{CT} changed

Table 1. Fitted EIS Parameters of the Symmetric Cells Based on Different Counter Electrodes

counter electrode	R_S/Ω cm^2	R_{CT}/Ω cm^2	N_P/Ω cm^2
PEDOT-1	21.57	6.19	8.56
PEDOT-2	20.18	1.33	1.62
PEDOT-3	20.67	2.24	2.39
Pt	19.22	0.64	N.A.

significantly from one CE to another. The PEDOT-2 CE showed the smallest R_{CT} (1.33 Ω cm^2) value among the three PEDOT CEs, close to that of the Pt CE (0.64 Ω cm^2). Meanwhile, these R_{CT} values are well below the 10 Ω cm^2 needed for high-performance DSCs, indicating that SSP-PEDOT electrodes can be utilized as efficient counter electrodes in the device.[37] In addition, N_P of PEDOT CEs varies with the loading amount in a similar way to R_{CT}. The variation of N_P reflected the change of Nernst diffusion impedance due to the diffusion of the electrolyte through the counter electrode pores. N_P has an influence on the photovoltaic performance of the device,[21,38] which will be discussed in more detail in the following section.

The CV and EIS results indicate that PEDOT electrodes prepared by the solid-state polymerization approach can be a potential counter electrode for high-performance DSCs. Consequently, the SSP-PEDOT electrodes with various loading amount of PEDOT were assembled with N719-sensitized TiO_2 electrodes to fabricate DSC devices. For comparison, the Pt-coated electrode, DBEDOT film and blank FTO were also utilized as the CEs in DSCs with N719-sensitized TiO_2 under the same conditions in control experiments. The photocurrent density−voltage characteristic curves of DSCs with various CEs measured under the illumination of 100 mW cm^{-2} AM 1.5 are shown in Figure 4. The corresponding photovoltaic parameters are summarized in Table 2. As expected, the devices based on

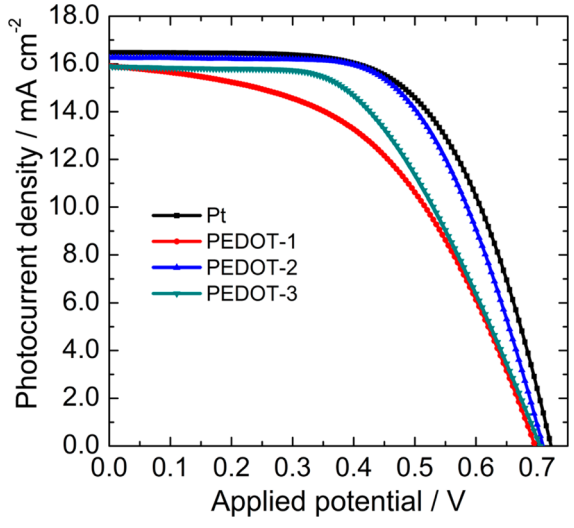

Figure 4. Characteristic photocurrent density−voltage (J−V) curves of the DSCs with different CEs based on the rigid FTO substrates, measured under solar simulator illumination (AM 1.5 100 mW cm^{-2}); the loading amount of PEDOT for PEDOT-1, PEDOT-2, and PEDOT-3 films is 1.5, 3.0, and 4.5 mg cm^{-2}, respectively.

Table 2. Photovoltaic Performances and EIS Parameters of the DSCs with Different CEs Measured under 1 sun Illumination (AM 1.5 100 mW cm^{-2})

device	V_{oc} (V)	J_{sc} (mA cm^{-2})	FF	η (%)	R_S (Ω)	R_{CT1} (Ω)	R_{CT2} (Ω)	R_{TOTAL} (Ω)
PEDOT-1	0.695	15.90	0.49	5.41	22.95	11.14	34.52	68.61
PEDOT-2	0.710	16.26	0.61	7.04	20.32	8.57	20.71	49.60
PEDOT-3	0.705	15.91	0.53	5.94	20.79	10.22	22.32	53.33
Pt	0.720	16.47	0.62	7.35	19.67	6.17	16.06	41.90

blank FTO or DBEDOT monomer film CE showed a very low power conversion efficiency of 0.02% (not shown here). The low efficiency is due to poor catalytic activity of CE on I_3^- reduction and subsequently poor regeneration of oxidized dye. Heating DBEDOT film at 80 °C for 6 h converted it to the conducting PEDOT film. As a result, the power conversion efficiency of the device based on PEDOT-1 film increased to 5.41%. The corresponding open-circuit voltage (V_{oc}), short-circuit photocurrent density (J_{sc}), and fill factor (FF) for the solar cell were 0.695 V, 15.90 mA cm^{-2}, and 0.49, respectively. A better power conversion efficiency was gained when the loading amount of PEDOT on the substrate increased from 1.5 to 3.0 mg cm^{-2}. The DSC based on the PEDOT-2 CE presented the highest conversion efficiency of 7.04% with V_{oc} of 0.710 V, J_{sc} of 16.26 mA cm^{-2}, and FF of 0.61, which is comparable with that of the Pt CE-based DSC device with conversion efficiency of 7.35%, V_{oc} of 0.720 V, J_{sc} of 16.47 mA cm^{-2}, and FF of 0.62. However, further increasing the loading amount to 4.5 mg cm^{-2} (PEDOT-3) resulted in decreased conversion efficiency (5.94%), mainly because of the decline of FF to 0.53. Clearly, the loading amount of PEDOT film has a great influence on the FF of the device and subsequently the conversion efficiency.

Furthermore, the effects of SSP-PEDOT CEs with different loading amount of PEDOT on the photovoltaic characteristics of DSCs can be investigated using EIS measured under light illumination.[39−43] The EIS spectra of DSCs with Pt CE and various SSP-PEDOT CEs are shown in Figure 5, and the equivalent circuit is shown in the inset.[39−43] In general, the EIS

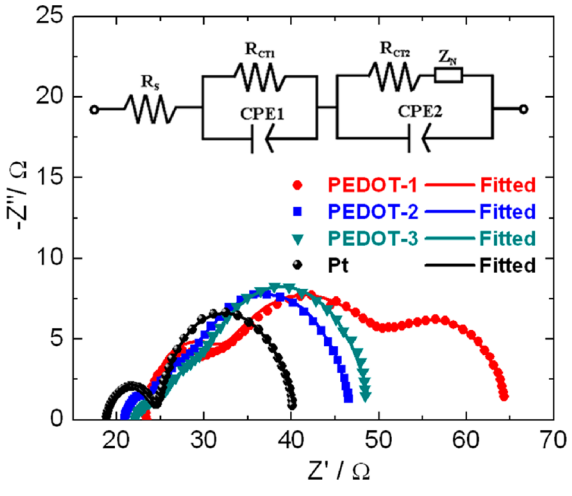

Figure 5. Electrochemical impedance spectra of DSCs using the SSP-PEDOT CEs with different loading amounts and Pt CE, measured under irradiation of 100 mW cm^{-2} AM 1.5 at open-circuit voltage. Inset shows the equivalent circuit for fitting; dots present experimental results; and solid lines show fitted results; the loading amount of PEDOT for PEDOT-1, PEDOT-2, and PEDOT-3 films is 1.5, 3.0, and 4.5 mg cm^{-2}, respectively.

of a DSC presents three characteristic semicircles in the scanning frequency range between 10^5 and 0.05 Hz. The high-frequency semicircle is related to the charge-transfer resistance at the interface of the counter electrode and the liquid electrolyte (R_{CT1}). The middle frequency semicircle is attributed to charge transfer and recombination at the TiO_2/dye/electrolyte interfaces (R_{CT2}). The low-frequency semicircle is ascribed to the Nernst diffusion of the I_3^-/I^- redox couple in the electrolyte (Z_N). In addition, R_S is defined as the substrate resistance, whose value is directly related to the sheet resistance of TCO.[39,40] As shown in Figure 5, only two main semicircles are observed for as-fabricated DSC devices using PEDOT-2 and PEDOT-3 and the Pt CE, and the third arc for Nernst diffusion is not obvious and overlapped by R_{CT2}. This is mainly due to the low viscosity of the liquid electrolyte used in the study.[41,42] However, the third semicircle is presented for the DSC device with the PEDOT-1 CE. The appearance of a larger semicircle at low frequency in the case of the PEDOT-1 CE is mainly related to the poor catalytic activity of the as-fabricated CE on the reduction of triiodide.[39−42] The corresponding fitted values of R_S, R_{CT1}, and R_{CT2} are also listed in Table 2. R_S values of all devices are close to each other, in accordance with the fact that all the devices were fabricated under similar conditions. R_{CT1}, which is determined by the diameter of the semicircle of the high-frequency region of impedance spectra, is related to the electrocatalytic performance of the CEs on the triiodide reduction.[39−43] R_{CT1} decreases with the increase of the loading amount of PEDOT on the substrate from 1.5 to 3.0 mg cm^{-2}. The R_{CT1} value for PEDOT-1 CE and PEDOT-2 CE was 11.14 and 8.57 Ω, respectively. As illustrated in Figure 3 and Table 1, the Nernst diffusion impedance (N_P) resulting from diffusion through the electrode pores largely decreased from 8.56 to 1.62 Ω cm^2 when the loading amount of PEDOT increased from 1.5 to 3.0 mg cm^{-2}. The change of N_P is related to the microstructure, effective surface area, and porosity of the CE. In general, a smaller value of R_{CT1} can lead to superior catalytic activity of the CE on the triiodide reduction. The improvement in catalytic activity of the PEDOT layer on triiodide reduction may be ascribed to the increase in the effective surface area and porosity in the thicker PEDOT films. The decrease in R_{CT1} can result in a higher FF and conversion efficiency.[14] However, with further increasing the loading amount of PEDOT to 4.5 mg cm^{-2}, the R_{CT1} increased to 10.22 Ω. The corresponding N_P changed to 2.39 Ω cm^2, implying that Nernst diffusion impedance enlarged for PEDOT-3 CE. The increase in R_{CT1} and N_P will show a negative effect on the catalytic activity of the CE. Therefore, further increasing the PEDOT loading will result in the decrease of photovoltaic performance. The R_{CT2} value for devices is related to the CEs used in the devices. Among these devices, the device with a Pt CE presents the smallest value of R_{CT2} (16.06 Ω), while the device with PEDOT-1 CE shows the largest value of R_{CT2} (34.52 Ω). Moreover, R_{CT2}, reflecting the properties of the photoinjected electrons within TiO_2, was found to be dependent on the

applied bias voltage. The V_{OC} and R_{CT2} for a device with PEDOT-2 CE are almost identical to those for the device with PEDOT-3 CE. The change in conversion efficiency is related to a change in the total internal resistance, which influences the photovoltaic performance of the DSC. As the DSCs generally operate under direct current conditions, the capacitances (CPE1 and CPE2) can be ignored. Therefore, the total internal series resistance (R_{TOTAL}) can be then described as[14,39,40]

$$R_{TOTAL} = R_S + R_{CT1} + R_{CT2} + Z_N \quad (3)$$

As the semicircle of Z_N was overlapped by the semicircle of R_{CT2}, the equation can be simply described as

$$R_{TOTAL} = R_S + R_{CT1} + R_{CT2} \quad (4)$$

The device with Pt CE presents a lower R_{TOTAL} (41.90 Ω) and higher-energy conversion efficiency than those of devices with SSP-PEDOT CEs. Among the PEDOT-based devices, R_{TOTAL} for devices based on SSP-PEDOT-1, PEDOT-2, and PEDOT-3 is 68.61, 49.60, and 53.33 Ω, respectively. The DSC containing PEDOT-2 CE shows the smallest R_{TOTAL} among the SSP-PEDOT-based devices. The decrease in R_{TOTAL} helps to improve the FF and conversion efficiency, and its conversion efficiency is very close to that of a DSC device with a Pt CE. To be specific, the enhanced photovoltaic performance of the device is mainly due to the large effective surface area, porosity, and thus the improved catalytic activity of the SSP-PEDOT CE. As a result, the PEDOT-2 CE-based DSC achieves an energy conversion efficiency of 7.04%, which is comparable with that of the Pt CE-based device (7.35%).

As mentioned above, the high-performance SSP-PEDOT film can be easily prepared via solid-state polymerization at 80 °C using the DBEDOT monomer. Therefore, one of the advantages of the SSP method is its applicability in the fabrication of PEDOT film on the plastic ITO/PEN substrates, which can only sustain temperature lower than 150 °C. With the optimized fabrication conditions for SSP-PEDOT CE on rigid FTO glass substrate, SSP-PEDOT electrodes were fabricated on a plastic PEN/ITO substrate. The photograph of the resultant plastic PEDOT electrode is shown in the inset of Figure 6. All-plastic DSCs were subsequently assembled with an N719-sensitized P25 TiO_2 electrode as the photoanode and SSP-PEDOT as the counter electrode. Its current density–voltage curve is plotted in Figure 6. The all-plastic DSC device exhibits a V_{oc} of 0.726 V, a J_{sc} of 11.90 mA cm^{-2}, and a FF of 0.54, which yield an energy conversion efficiency of 4.65%. The results also confirm that the PEDOT CEs fabricated via solid-state polymerization using DBEDOT monomer can be easily incorporated onto the plastic substrate. For comparison, an all-plastic DSC consisting of a N719-sensitized P25 TiO_2 electrode and sputter-deposited Pt CE was also prepared under the same conditions. The corresponding photocurrent density–voltage curve is also shown in Figure 6. The photovoltaic parameters of a DSC with sputter-deposited Pt CE are 0.724 V (V_{oc}), 12.83 mA cm^{-2} (J_{sc}), 0.58 (FF), and 5.38% (η), respectively. The photovoltaic characteristics of all-plastic DSC devices also demonstrate that the PEDOT CE fabricated via solid-state polymerization using the DBEDOT monomer has shown a catalytic property for triiodide reduction comparable with that of the Pt CE prepared using a sputtering technique. Moreover, it also indicates that solid-state polymerization of DBEDOT is an efficient low-cost method to fabricate a highly efficient CE at low temperature for plastic DSC devices.

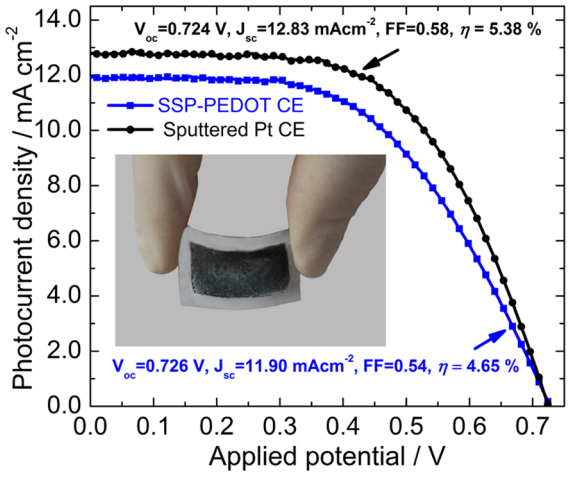

Figure 6. Photovoltaic characteristics of plastic DSCs with plastic sputter-deposited Pt CE and plastic SSP-PEDOT CE, measured under irradiation of 100 mW cm^{-2} AM 1.5; inset shows the photograph of the plastic SSP-PEDOT CE.

CONCLUSION

In conclusion, a low-cost, low-temperature method to fabricate the high-performance PEDOT CEs for plastic dye-sensitized solar cells has been successfully developed via a facile solid-state polymerization at 80 °C for 6 h with DBEDOT monomer as the starting material. The optimal SSP-PEDOT CE-based rigid DSC and plastic DSC presented a power conversion efficiency of 7.04% and 4.65%, respectively, which are comparable with the values obtained from the devices based on a thermally deposited Pt CE (7.35%) and sputter-deposited Pt CE (5.38%). The superior performance indicates that PEDOT film synthesized via a low-temperature solid-state polymerization is a promising CE material for high-performance Pt-free plastic DSCs.

AUTHOR INFORMATION

Corresponding Author

*E-mail: mhe@nanoctr.cn (M. He). Tel.: +86 10 8254 5555. Fax: +86 10 62656765. E-mail: linyuan@iccas.ac.cn (Y. Lin). Tel.: +86 10 8261 5031. Fax: +86 10 8261 7315.

Author Contributions

‖These authors contributed equally.

Notes

The authors declare no competing financial interest.

ACKNOWLEDGMENTS

The work was financially supported by the Major State Basic Research Development Program of China (973 Program) (No. 2011CB932702) and the National Natural Science Foundation of China (Grant Nos. 21103032, 51272049, 21071016). We also thank Dr. J. B. Shi for help in preparation of the thiophene monomer.

REFERENCES

(1) O'Regan, B.; Grätzel, M. *Nature* **1991**, *353*, 737–740.
(2) Hagfeldt, A.; Boschloo, G.; Sun, L. C.; Kloo, L.; Pettersson, H. *Chem. Rev.* **2010**, *110*, 6595–6663.
(3) Grätzel, M. *Nature* **2001**, *414*, 338–344.
(4) Yella, A.; Lee, H.-W.; Tsao, H. N.; Yi, C. Y.; Chandiran, A. K.; Nazeeruddin, Md. K.; Diau, E. W.-G.; Yeh, C.-Y.; Zakeeruddin, S. M.; Grätzel, M. *Science* **2011**, *334*, 629–634.

(5) Horiuchi, T.; Miura, H.; Sumioka, K.; Uchida, S. *J. Am. Chem. Soc.* **2004**, *126*, 12218−12219.
(6) Qin, H.; Wenger, S.; Xu, M.; Gao, F.; Jing, X.; Wang, P.; Zakeeruddin, S. M.; Grätzel, M. *J. Am. Chem. Soc.* **2008**, *130*, 9202−9203.
(7) Nazeeruddin, M. K.; Kay, A.; Rodicio, I.; Humpbry-Baker, R.; Miiller, E.; Liska, P.; Vlachopoulos, N.; Grätzel, M. *J. Am. Chem. Soc.* **1993**, *115*, 6382−6390.
(8) Papageorgiou, N. *Coord. Chem. Rev.* **2004**, *248*, 1421−1446.
(9) Wu, M. X.; Ma, T. L. *ChemSusChem* **2012**, *5*, 1343−1357.
(10) Olsen, E.; Hagen, G.; Lindquist, S.-E. *Sol. Energy Mater. Sol. Cell* **2000**, *63*, 267−273.
(11) Jo, Y.; Cheon, J. Y.; Yu, J.; Jeong, H. Y.; Han, C.-H.; Jun, Y.; Joo, S. H. *Chem. Commun.* **2012**, *48*, 8057−8059.
(12) Dong, P.; Pint, C. L.; Hainey, M.; Mirri, F.; Zhan, Y. J.; Zhang, J.; Pasquali, M.; Hauge, R. H.; Verduzco, R.; Jiang, M.; Lin, H.; Lou, J. *ACS Appl. Mater. Interfaces* **2011**, *3*, 3157−3161.
(13) Guai, G. H.; Leiw, M. Y.; Ng, M. C.; Li, C. M. *Adv. Energy Mater.* **2012**, *2*, 334−338.
(14) Yin, X.; Xue, Z. S.; Liu, B. *J. Power Sources* **2011**, *196*, 2422−2426.
(15) Yin, X.; Liu, X. Z.; Wang, L.; Liu, B. *Electrochem. Commun.* **2010**, *12*, 1241−1244.
(16) Yin, X.; Xue, Z. S.; Wang, L.; Cheng, Y. M.; Liu, B. *ACS Appl. Mater. Interfaces* **2012**, *4*, 1709−1715.
(17) Xue, Z. S.; Zhang, W.; Yin, X.; Cheng, Y. M.; Wang, L.; Liu, B. *RSC Adv.* **2012**, *2*, 7074−7080.
(18) Fu, N.-Q.; Fang, Y.-Y.; Duan, Y.-D.; Zhou, X.-W.; Xiao, X.-R.; Lin, Y. *ACS Nano* **2012**, *6*, 9596−9605.
(19) Weerasinghe, H. C.; Huang, F. Z.; Cheng, Y.-B. *Nano Energy* **2013**, *2*, 174−189.
(20) Sudhagar, P.; Nagarajan, S.; Lee, Y.-G.; Song, D.; Son, T.; Cho, W.; Heo, M.; Lee, K.; Won, J.; Kang, Y. S. *ACS Appl. Mater. Interfaces* **2011**, *3*, 1838−1843.
(21) Xu, H. X.; Zhang, X. Y.; Zhang, C. J.; Liu, Z. H; Zhou, X. H.; Pang, S. P.; Chen, X.; Dong, S. M.; Zhang, Z. Y.; Zhang, L. X.; Han, P. X.; Wang, X. G.; Cui, G. L. *ACS Appl. Mater. Interfaces* **2012**, *4*, 1087−1092.
(22) Yun, S. N.; Wang, L.; Guo, W.; Ma, T. L. *Electrochem. Commun.* **2012**, *24*, 69−73.
(23) Xue, Y. H.; Liu, J.; Chen, H.; Wang, R. G.; Li, D. Q.; Qu, J.; Dai, L. M. *Angew. Chem., Int. Ed.* **2012**, *51*, 12124−12127.
(24) Roy-Mayhew, J. D.; Boschloo, G.; Hagfeld, A.; Aksay, I. A. *ACS Appl. Mater. Interfaces* **2012**, *4*, 2794−2800.
(25) Veerappan, G.; Bojan, K.; Rhee, S.-W. *ACS Appl. Mater. Interfaces* **2011**, *3*, 857−862.
(26) Pringle, J. M.; Armel, V.; MacFarlane, D. R. *Chem. Commun.* **2010**, *46*, 5367−5369.
(27) Trevisan, R.; DÖbbelin, M.; Boix, P. P.; Barea, E. M.; Tena-Zaera, R.; Nora-SerÓ, I.; Bisquert, J. *Adv. Energy Mater.* **2011**, *1*, 781−784.
(28) Xia, J. B.; Masaki, N.; Jiang, K. J.; Yanagida, S. *J. Mater. Chem.* **2007**, *17*, 2845−2850.
(29) Groenendaal, L. B.; Jonas, F.; Freitag, D.; Pielartzik, H.; Reynolds, J. R. *Adv. Mater.* **2000**, *12*, 481−494.
(30) Shin, H.-J.; Jeon, S. S.; Im, S. S. *Synth. Met.* **2011**, *161*, 1284−1288.
(31) Lee, K.-M.; Chiu, W.-H.; Wei, H.-Y.; Hu, C.-W.; Suryanarayanan, V.; Hsien, W.-F.; Ho, K.-C. *Thin Solid Films* **2010**, *518*, 1716−1721.
(32) He, M.; Okudera, H.; Simon, A.; Köhler, J.; Jin, S. F.; Chen, X. L. *J. Solid State Chem.* **2013**, *197*, 466−470.
(33) He, M.; Okudera, H.; Simon, A. *Inorg. Chem.* **2005**, *44*, 4421−4426.
(34) Meng, H.; Perepichka, D. F.; Bendikov, M.; Wudl, F.; Pan, G. Z.; Yu, W. J.; Dong, W. J.; Brown, S. *J. Am. Chem. Soc.* **2003**, *125*, 15151−15162.
(35) Meng, H.; Perepichka, D. F.; Wudl, F. *Angew. Chem., Int. Ed.* **2003**, *42*, 658−661.
(36) Sotzing, G. A.; Reynolds, J. R. *Chem. Mater.* **1996**, *8*, 882−889.
(37) Hauch, A.; Georg, A. *Electrochim. Acta* **2001**, *46*, 3457−3466.
(38) Roy-Mayhew, J. D.; Bozym, D. J.; Punckt, C.; Aksay, I. A. *ACS Nano* **2010**, *10*, 6203−6211.
(39) Han, L. Y.; Koide, N.; Chiba, Y.; Islam, A.; Komiya, R.; Fukui, N.; Yamanaka, R. *Appl. Phys. Lett.* **2005**, *86*, 213105.
(40) Han, L. Y.; Koide, N.; Chiba, Y.; Mitate, T. *Appl. Phys. Lett.* **2004**, *84*, 2433.
(41) Fabregat-Santiago, F.; Bisquert, J.; Palomares, E.; Otero, L.; Kuang, D.; Zakeeruddin, S. M.; Grätzel, M. *J. Phys. Chem. C* **2007**, *111*, 6550−6560.
(42) Lin, L.-Y.; Nien, P.-C.; Lee, C.-P.; Tsai, K.-W.; Yeh, M.-H.; Vittal, R.; Ho, K.-C. *J. Phys. Chem. C* **2010**, *114*, 21808−21815.
(43) Fu, N.-Q.; Xiao, X.-R.; Zhou, X.-W.; Zhang, J.-B.; Lin, Y. *J. Phys. Chem. C* **2012**, *116*, 2850−2857.